Are There Fundamental Limitations on the Sheet Resistance and Transmittance of Thin Graphene Films?

Sukanta De and Jonathan N. Coleman*

School of Physics and CRANN, Trinity College Dublin, Dublin 2, Ireland

ABSTRACT From published transmittance and sheet resistance data, we have calculated a figure of merit for transparent, conducting graphene films; the DC to optical conductivity ratio, σ_{DC}/σ_{Op}. For most reported results, this conductivity ratio clusters around the values $\sigma_{DC}/\sigma_{Op} = 0.7$, 4.5, and 11. We show that these represent fundamental limiting values for networks of graphene flakes, undoped graphene stacks, and graphite films, respectively. The limiting value for graphene flake networks is much too low for transparent-electrode applications. For graphite, a conductivity ratio of 11 gives $R_s = 377\Omega/\square$ for $T = 90\%$, far short of the 10 $\Omega/\square$ minimum requirement for transparent conductors in current driven applications. However, we suggest that substrate-induced doping can potentially increase the 2-dimensional DC conductivity enough to make graphene a viable transparent conductor. We show that four randomly stacked graphene layers can display T $\approx$ 90% and 10 $\Omega/\square$ if the product of carrier density and mobility reaches $n\mu = 1.3 \times 10^{17}$ V^{-1} s^{-1}. Given achieved doping values and attainable mobilities, this is just possible, resulting in potential values of σ_{DC}/σ_{Op} of up to 330. This is high enough for any transparent conductor application.

KEYWORDS: transparent · conductor · electrode · graphene · figure of merit

Transparent electrodes are essential to many areas of modern electronics and are commonly found in displays, touch-panels, light emitting diodes, and solar cells.[1] However, the cost of the standard material used, indium tin oxide (ITO), is increasing rapidly owing to supply and demand issues. Potential replacement materials include alternative metal oxides,[2,3] thin metal films,[4,5] or metal grids.[6,7] To replace ITO, it is generally agreed that such materials must, at the very least, display a sheet resistance of $R_s < 100$ $\Omega/\square$, coupled with transmittance of $T > 90\%$ in the visible.[8−10] However, for some current driven applications such as solar cells and light emitting diodes, even lower sheet resistances are required. In flat panel displays, the transparent data lines must have $R_s <$ 20 $\Omega/\square$, to provide acceptable RC delays.[11] Devices with large pixels also require low sheet resistance. Larger pixels result in higher power losses which can only be reduced by lowering sheet resistance.[12] In the latter case $R_s \approx 10$ $\Omega/\square$ is necessary.[12−14] ITO is commercially available with sheet resistance as low as ~10 $\Omega/\square$ for a transmittance of ~85%. Thus, any potential ITO replacement must match these properties ($R_s \approx 10$ $\Omega/\square$ and T $\approx$ 85%). In addition, future displays will be larger than in the past and will probably reside on plastic rather than glass and so must be flexible. Thus, prospective displays will require flexible transparent electrodes that can be produced at low temperature and over large areas at low cost. Neither ITO nor the alternatives mentioned above have these qualities. We note that such requirements are *in addition to* traditional technical requirements associated with low sheet resistance and high transparency.

It has been known for the past few years that flexibility and low temperature processing can be achieved by the deposition of nanostructured thin films, often from the liquid phase. These are known to be stable under flexing[15] and can be spray cast,[9] opening the way to large area deposition. While polymer[16] and metal nanowire films[17,18] have been studied recently, possibly the most common nanomaterial used to date has been carbon nanotubes.[9,15,19,20] While networks of both metallic nanowires[18] and carbon nanotubes[21] have the properties to potentially replace ITO, both materials are extremely expensive (in the two papers cited above, the nanomaterials cost $3000/g and $1600/g, respectively). As a result many researchers have turned to graphene.[22−47] Among its many exciting properties,[48,49] graphene is conductive and, when stacked thin enough, can be transparent. In addition, it can be exfoliated in water as graphene oxide[50] or as pristine graphene in solvents[31,51−54] or using

*Address correspondence to colemaj@tcd.ie.

Received for review February 19, 2010 and accepted March 31, 2010.

Published online April 12, 2010.
10.1021/nn100343f

surfactants.[30,41,55] These exfoliated dispersions can be used to prepare thin, transparent, conducting films. Alternatively graphene films can be grown by chemical vapor deposition (CVD).[28,56] Such films have demonstrated reasonably impressive opto-electrical properties; for example sheet resistances of $R_s = 200\Omega/\square$ coupled with transmittances of $T = 85\%$ (550 nm).[38] However, they have fallen well short of the results achieved for carbon nanotubes or silver nanowires.

A number of issues make it difficult to accurately assess progress in this area. In the vast majority of cases, researchers only report values of T (usually at 550 nm) and R_s for their films. As the reported films tend to have different thickness, comparison between films is difficult. In some cases, the film thicknesses are measured and the DC conductivity reported. However, intrinsic measures of the light absorption in the films are rarely reported. In addition, figures of merit (FoMs) for transparent conductors are hardly ever reported. This is a serious problem as FoMs represent the only reliable way to compare properties with other graphitic films or indeed with transparent conductors made from other materials. Finally, and possibly most seriously, comparisons are almost never made with the industry requirements for transparent electrodes.

In this letter, we address these issues by analyzing data from the literature on graphene-based transparent conducting films. We identify an appropriate figure of merit, the DC to optical conductivity ratio, and calculate it for all papers analyzed. We rank the data by this FoM and analyze whether the rankings are determined by the DC or optical conductivity. We make estimates for the upper limits on the FoM for graphitic films and films of undoped graphene monolayers (or randomly stacked monolayers) and show that these limits have already been reached. These upper limits are not good enough to make graphite or undoped garphene a viable material for transparent electrodes. However, we show that substrate-induced doping can increase the DC conductivity enough to make graphene a viable candidate for transparent electrodes in display applications.

DISCUSSION

Published Data for Transmittance and Sheet Resistance. The published data for T and R_s of graphene films shows a very large variation from highly conductive films to films with relatively high resistances. We have analyzed >20 papers in the literature on transparent, conducting graphitic films, focusing on T and R_s. Shown in Figure 1 are the data extracted from these papers (see Supporting Information, Table 1) plotted as *T versus* R_s. It is clear from this graph that sheet resistances vary from a few hundred ohms per square to greater than $10^5\ \Omega/\square$. Clearly, there is a need to understand the variation between these films and the factors which limit the opto-electrical properties of such films.

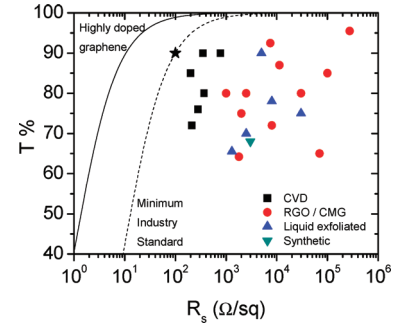

Figure 1. Transmittance and sheet resistance data for papers appearing in the literature. These are broken down into films prepared by CVD, or from reduced graphene oxide or chemically modified graphene, pristine exfoliated graphene, or chemically synthesized graphene. In all cases the data in the figure correspond to the best data reported. The star represents the minimum industry standard for transparent electrodes ($R_s = 100\ \Omega/\square$, $T = 90\%$). This corresponds to $\sigma_{DC}/\sigma_{Op} = 35$. The dashed line illustrates the set of (T, R_s) data consistent with $\sigma_{DC}/\sigma_{Op} = 35$. The solid line corresponds to the calculated case of highly doped graphene ($\sigma_{DC}/\sigma_{Op} = 330$).

To analyze transmittance and sheet resistance data for transparent conducting films, it is important to note that R_s and T are in fact linked. Both are determined by the response of electrons to either static (voltage) or dynamic (light) electric fields. The sheet resistance is ultimately controlled by the (3-dimensional) DC conductivity, σ_{DC}, *via*

$$R_s = (\sigma_{DC} t)^{-1} \tag{1}$$

where t is the film thickness. The transmittance is controlled by the optical conductivity, σ_{Op}, *via*[57]

$$T = \left(1 + \frac{Z_0}{2}\sigma_{Op} t\right)^{-2} \tag{2}$$

where Z_0 is the impedance of free space and has the value 377 Ω. We note that the optical conductivity is related to the Lambert−Beer absorption coefficient, α, by $\sigma_{Op} \approx 2\alpha/Z_0$.[58] We can combine these equations, eliminating t, to give a relationship between T and R_s for a thin conducting film:

$$T = \left(1 + \frac{Z_0}{2R_s}\frac{\sigma_{Op}}{\sigma_{DC}}\right)^{-2} \tag{3}$$

Thus, the relationship between T and R_s is controlled by the conductivity ratio, σ_{DC}/σ_{Op}. This parameter can then be used as a FoM. High values of σ_{DC}/σ_{Op} result in the desired properties (high T, low R_s).

The minimum industry standard for ITO replacement materials is a sheet resistance of $R_s < 100\ \Omega/\square$ coupled with transmittance of $T > 90\%$ in the visible. Using eq 3, this means $\sigma_{DC}/\sigma_{Op} > 35$. However, for most current driven applications, the more stringent condition of $R_s < 10\ \Omega/\square$ (@$T = 85\%$) is necessary. This results in the condition that $\sigma_{DC}/\sigma_{Op} > 220$. In this paper we will compare the values of σ_{DC}/σ_{Op} calculated from the literature with these industry standards.

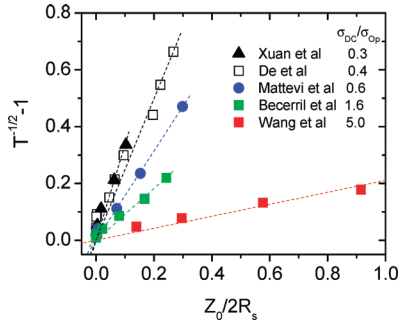

Figure 2. *T* and R_s data for thin films of graphene flakes plotted to show the applicability of eq 3. When plotted this way, the slope of the curves is equal to $(\sigma_{DC}/\sigma_{Op})^{-1}$.

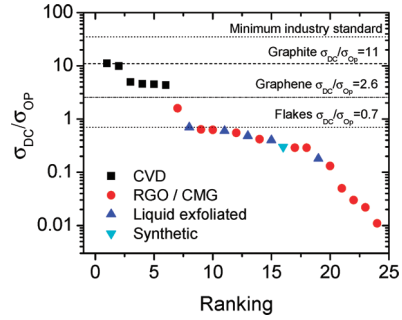

Figure 3. The conductivity ratio, σ_{DC}/σ_{Op}, as calculated from *T* and R_s data reported in the literature. This data has been ranked from highest (1) to lowest (24). The horizontal lines indicate specific values of σ_{DC}/σ_{Op}. The top line represents the minimum industry standard (σ_{DC}/σ_{Op} = 35). The other lines represent fundamentally limiting values of σ_{DC}/σ_{Op} for (top to bottom) graphite thin films, undoped graphene films, and thin films consisting of graphene flakes.

We will use eq 3 to calculate σ_{DC}/σ_{Op} from the R_s, *T* data reported in over 20 published works. However, first we must demonstrate its applicability. We took R_s and *T* data from the literature[39−41,45,46] for graphene films of varying thickness. We recast the data as $T^{-1/2} - 1$ and $Z_0/2R_s$. According to eq 3, these quantities should scale linearly. This data is plotted in Figure 2 and demonstrates the validity of eq 3. We note that this expression has also been shown to fit well to data for films of carbon nanotubes,[15] silver nanowires,[18] and polymer−nanotube composites.[59] (This equation tends to work less well at low thickness for all nanostructured films. This is due to the finite thickness of the structures making the film[15,18,41,59]).

Calculated Conductivity Ratio for Published Data. We have calculated σ_{DC}/σ_{Op} from the R_s, *T* data reported in more than 20 papers (see Supporting Information for data and ranking). If more than one system was presented (*i.e.*, as-produced and annealed films) we generally report only the higher value. We have ranked these values from highest to lowest value of σ_{DC}/σ_{Op}. We have categorized the samples by graphene type: (1) CVD grown graphene, (2) reduced graphene oxide or chemically modified graphene (RGO/CMG), (3) pristine, liquid-exfoliated graphene, and (4) synthetically grown graphene. We note that for categories 2 and 3, both films are processed from solution. Shown in Figure 3 are the σ_{DC}/σ_{Op} data plotted *versus* ranking. A number of things are immediately apparent: The data is spread over three decades of σ_{DC}/σ_{Op} values and CVD films are clearly the best while solution processed films are poorer in quality and span a wider range. Interestingly, there appear to be three plateaux in the data, at $\sigma_{DC}/\sigma_{Op} \approx 0.7$, $\sigma_{DC}/\sigma_{Op} \approx 4.5$ and $\sigma_{DC}/\sigma_{Op} \approx 10$. We will return to these plateaux later.

Given the large range of σ_{DC}/σ_{Op} data, one must ask whether variations in σ_{DC} or σ_{Op} are responsible for the spread. Film thicknesses were given in about half of the papers studied. This allows us to calculate both σ_{DC} and σ_{Op} using eqs 1 and 2. These data are shown in Figure 4, plotted against the same overall ranking used in Figure 3. We see from Figure 4A that σ_{Op} varies randomly from 10^4 to 2×10^5 S/m (median 6.8×10^4 S/m). The optical conductivity is controlled by the intrinsic properties of the flakes[60] and the number of flakes per volume. We suggest that the variation in σ_{Op} is due to film-to-film differences in morphological properties such as density. However, σ_{DC} tends to decrease significantly in the direction of poorer rankings, varying by over 2 orders of magnitude. This tells us that the variation in σ_{DC}/σ_{Op} is primarily controlled by the variation in σ_{DC}. This relatively large variation in σ_{DC} means that the factors controlling current flow vary strongly from film to film. By analogy with nanotube networks,[21,61] we expect the most important factor affecting current

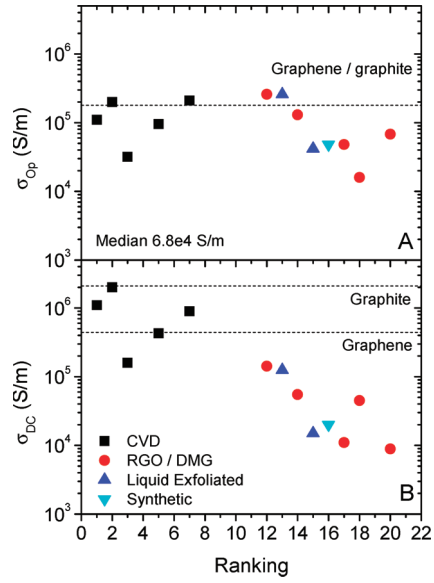

Figure 4. The optical (A) and DC (B) conductivities calculated for the films presented in the literature. Note that the ranking is the same as that in Figure 3. However, we could only calculate σ_{DC} and σ_{Op} in the cases where the film thickness was given (or could be calculated from the presented data). The horizontal line in Figure 4A represents the theoretical (and measured) value for the optical conductivity of films consisting of stacked graphene layers. The upper horizontal line in Figure 4B represents the DC conductivity of graphite. The lower horizontal line represents the DC conductivity of undoped graphene (estimated from the 2D conductivity of graphene divided by the layer thickness).

flow is the presence/absence and quantity of interflake tunnelling barriers. We would expect very few tunnelling barriers in the quasi-continuous CVD grown films. However the quantity of barriers should vary greatly in the solution-deposited films, due to variations in flake size and degree of aggregation/exfoliation. This effect is manifested by the fact that the CVD samples are in the region of the upper and middle plateaux in Figure 3 while the solution cast films (RGO/CMG and liquid-exfoliated) are on or below the lower plateau. Interestingly, the RGO/CMG and pristine liquid-exfoliated graphene films are distributed rather evenly over the lower part of the curve. This fact, that these two classes of material are not well differentiated, shows that the defects common to RGO/CMG flakes[62] do not limit the conductivity. This confirms that the conductivity is limited by interflake junctions in both material types.

Limiting Values of σ_{DC}/σ_{Op}. We are now in a position to consider limiting values for σ_{DC}/σ_{Op}. It can be seen from Figure 1 that the data can be divided into that for quasi-continuous CVD grown films and networks of liquid-deposited small flakes. We will consider the latter case first.

Solution-Cast Graphene Networks. The DC conductivity and so σ_{DC}/σ_{Op} of graphene networks will be limited by interflake junctions. By analogy with nanotube networks, we expect the conductivity to be maximized for highly exfoliated systems.[61] The effect of exfoliation in graphene networks has recently been studied. Green *et al*. separated surfactant exfoliated graphene flakes by thickness using density gradient centrifugation.[30] They measured the flake size and thickness by AFM before making films and measuring T and R_s. They observed that thinner flakes gave better T and R_s values. We have calculated σ_{DC}/σ_{Op} for their data, plotting it *versus* flake thickness as shown in Figure 5A. This clearly shows the value of exfoliation with σ_{DC}/σ_{Op} increasing to 0.6 for a mean flake thickness of 1.1 nm. Given that individual graphene monolayers appear to be ~1 nm thick when measured by AFM,[63] we can extrapolate this data to suggest that a completely exfoliated film of these flakes would have $\sigma_{DC}/\sigma_{Op} \approx 0.7$. Of course, this value will depend on the lateral flake size. However, the flakes in this study were a few hundred nm in size, typical for solution-exfoliated graphene. Thus we suggest that $\sigma_{DC}/\sigma_{Op} \approx 0.7$ may be close to the limiting value for networks of liquid-exfoliated flakes. We note that $\sigma_{DC}/\sigma_{Op} \approx 0.7$ is exactly where the lower plateau occurs in Figure 3. We propose that this value is controlled by the topology of the network and the tunnelling probability between overlapping graphene sheets. Thus, for practical purposes, solution processed graphene cannot give films with σ_{DC}/σ_{Op} much greater than 0.7. We note that one paper on liquid-exfoliated films has reported a value of σ_{DC}/σ_{Op} slightly greater than 0.7.[40] At present, the reason for this discrepancy is unclear.

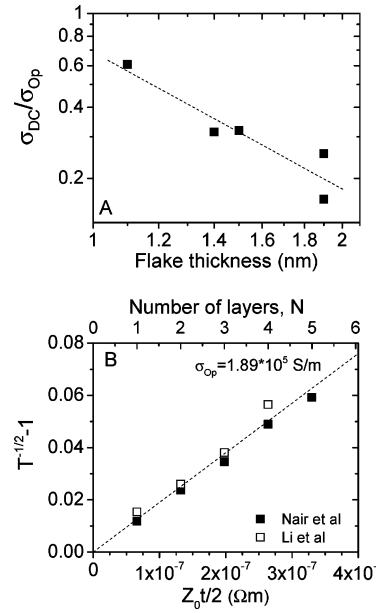

Figure 5. (A) Data calculated from Green and Hersam showing the scaling of σ_{DC}/σ_{Op} with flake thickness. In this work the flakes were separated by density gradient centrifugation. In all cases the flakes had lateral sizes of up to ~200 nm. This is typical of liquid-exfoliated graphene. (B) Data based on the transmittance, T, of multilayer graphene as a function of layer number, N, as published by Li *et al*. and Nair *et al*. We assume the multilayer thickness is $t = N \times 0.35$ nm. These data are plotted to show the applicability of eq 2. The slope of this graph is the (3-dimensional) optical conductivity of the multilayers. This works out to be close to 1.9×10^5 S/m for both data sets.

Monolayer or Randomly Stacked Graphene. The previous discussion was purely empirical. However, one can consider a theoretical limit for σ_{DC}/σ_{Op} in monolayer graphene films. Both the 2-dimensional DC (static) and optical (dynamic) conductivities of graphene monolayers are known[60,64,65] and take on the quantized values of: $\sigma_{2D,DC} = 4e^2/h$ and $\sigma_{2D,Op} = e^2/4\hbar$, respectively. However, we must remember that graphene is a two-dimensional object while we have been working with three-dimensional quantities (σ_{DC} and σ_{Op}). We suggest that the conductivity ratio in three dimensions (σ_{DC}/σ_{Op}) is just equal to the ratio of 2-dimensional DC conductivity to the 2-dimensional optical conductivity:

$$\frac{\sigma_{DC}}{\sigma_{Op}} = \frac{\sigma_{2D,DC}}{\sigma_{2D,Op}} = \frac{4e^2/h}{e^2/4\hbar} = \frac{8}{\pi} = 2.55 \qquad (4)$$

This represents an upper value for σ_{DC}/σ_{Op} for a pristine graphene monolayer or indeed for a stack of weakly interacting monolayers (*i.e.*, randomly stacked monolayers[66]). We have marked this value of σ_{DC}/σ_{Op} on Figure 3 as the third horizontal line from the top. We note that this line is just under a factor of 2 below the middle plateau. It is possible that the middle plateau represents quasi-continuous films consisting of weakly interacting (perhaps randomly stacked) graphene monolayers. In fact three of the four papers (ranking 3, 5, 6) associated with the middle plateau give electron

diffraction evidence of incommensurate layer stacking.[28,42,46] Such randomly stacked layers are expected to retain elements of their monolayer nature.[66] If, due to the weak intersheet interaction, the average intersheet distance was larger than $d = 0.35$ nm, this would manifest itself as a reduced value of σ_{Op} and so an increased value of σ_{DC}/σ_{Op} in line with the observed behavior. Alternatively, substrate-induced doping (see below) may be responsible for an increased conductivity. In fact, the fourth ranked film did indeed display evidence that the Fermi energy had been shifted from the neutrality point.[23] Interestingly, this results in a 2-dimensional conductivity which is a factor of 2 above its minimum value, in good agreement with the observed discrepancy.

Continuous Graphite Films. However, from Figure 3 there is clear evidence of another plateau appearing at higher values of $\sigma_{DC}/\sigma_{Op} \approx 10$. These higher values are harder to explain using doping or random stacking arguments. We note that the samples ranked 1 and 2 tend to have very high values of DC conductivity: $\sigma_{DC} > 10^6$ S/m. This is hard to rationalize with graphene. We can associate a 3-dimensional DC conductivity with graphene by dividing $\sigma_{2D,DC}$ by the layer thickness, $d = 0.35$ nm, in analogy with eq 1. This gives a value of $\sigma_{DC} = 4e^2/hd = 4.4 \times 10^5$ S/m. This value is plotted on Figure 4B for reference and is significantly below the values displayed by the top-ranked films. We can explain this apparent paradox by noting that single crystal graphite has a σ_{DC} value considerably larger than that just calculated for monolayer graphene.

We can consider the ultimate limitations for quasi-continuous graphitic films, such as those prepared by CVD, by modeling them as consisting of single crystal graphite. We will consider σ_{DC} and σ_{Op} separately for such films. Single crystal graphite can display in-plane conductivity as high as 2×10^6 S/m.[67,68] We note that this value (dashed line in Figure 4B) represents an effective upper limit for the conductivity of the films reported in the literature. We now turn to the optical conductivity of graphite. Recently, two papers have presented data for the optical transmittance of multilayer graphene as a function of the number of layers, N.[29,60] Modeling the thickness, t, of the multilayer as $t = Nd$, where $d = 0.35$ nm, we can use eq 2 to calculate σ_{DC}/σ_{Op} from the published data. We plot $T^{-1/2} - 1$ *versus* $Z_0 t/2$ in Figure 5B for both these data sets. Good overlapping straight lines are found, in both cases giving $\sigma_{Op} = 1.9 \times 10^5$ S/m. (This value is almost identical to the optical conductivity calculated by dividing the 2-dimensional optical conductivity[60] of graphene by the interlayer spacing d: $\sigma_{Op} = e^2/4\hbar d = 1.7 \times 10^5$ S/m). We note from Figure 4A that CVD films tend to have σ_{Op} close to this value (dashed line) while the solution processed films have lower values of σ_{Op}. This is consistent with solution cast films having significant free volume and so a density lower than that of graphite.

Knowledge of both σ_{DC} and σ_{Op} for graphite allows us to suggest that, for single crystalline graphite, $\sigma_{DC}/\sigma_{Op} = 11$ in the in-plane direction. This represents an upper limit, as any real graphitic film will have grain boundaries which will act to reduce σ_{DC}/σ_{Op}. We note that the upper plateau in Figure 3 lies very close to $\sigma_{DC}/\sigma_{Op} = 11$. This suggests that these films are close to single crystals. This is supported by high resolution TEM images for the first ranked film showing it to be highly crystalline.[38]

The discussion above suggests that it is impossible to prepare graphitic films with $\sigma_{DC}/\sigma_{Op} > 11$. This relatively low value is in spite of the high DC conductivities of the films prepared by Cai *et al.*[38] and Li *et al.*[29] which approach 2×10^6 S/m. These compare very favorably with the most conductive nanotube films which had $\sigma_{DC} \approx 5 \times 10^5$ S/m.[20,21] (Although we note that silver nanowire networks have displayed $\sigma_{DC} \approx 5 \times 10^6$ S/m.[18]) However, these high DC conductivities must be balanced against the optical conductivity. The value of $\sigma_{Op} = 1.8 \times 10^5$ S/m is among the highest of any material and compares unfavorably with those of carbon nanotube ($\sigma_{Op} = 1.7 \times 10^4$ S/m)[15] and silver nanowire networks ($\sigma_{Op} = 6472$ S/m).[18] It is this high optical conductivity which is responsible for the low conductivity ratio.

Beating the Limit by Doping. However, this does not mean that graphene-based films can never display $\sigma_{DC}/\sigma_{Op} > 11$. The quantized expression for 2-dimensional DC conductivity given in eq 4 refers to pristine monolayer graphene and is appropriate when the Fermi energy is at the Dirac point.[49] However, the Fermi energy can be shifted away from the Dirac point, either by applying a gate voltage or by doping. In this scenario, the 2-dimensional conductivity is no longer described by its quantized value but depends on the level of doping: $\sigma_{2D,DC} = ne\mu$, where n is the carrier density (electrons or holes) and μ is the carrier mobility.[64] It is well-known that inadvertent doping of graphene can occur when graphene is deposited on certain substrates.[23,28,31,63,69−71] Thus, we can anticipate realistic circumstances where graphene monolayers, or indeed randomly stacked graphene monolayers, can display large values of σ_{DC}/σ_{Op}. When doped, we can write the conductivity ratio as

$$\frac{\sigma_{DC}}{\sigma_{Op}} = \frac{ne\mu}{e^2/4\hbar} = \frac{4\hbar n\mu}{e} \qquad (5)$$

Thus to compete with ITO and to achieve $R_s < 100$ Ω/□ and $T > 90\%$ ($\sigma_{DC}/\sigma_{Op} > 35$), it will be necessary to dope graphene to a level consistent with $n\mu > 1.3 \times 10^{16}$ V^{-1} s^{-1}. To achieve the more stringent requirements of current driven devices ($R_s < 10$ Ω/□, $T > 85\%$, $\sigma_{DC}/\sigma_{Op} > 220$), $n\mu > 8.2 \times 10^{16}$ V^{-1} s^{-1} is required.

Blake *et al.* have shown that, when coated with polyvinyl alcohol (PVA), monolayer graphene is *n*-doped to

a level of $n = 3 \times 10^{12}$ cm^{-2}.[31] It is likely that this level of doping could be achieved in a working device by coating the substrate with a thin, transparent layer of PVA. In addition, monolayer graphene displays very high carrier mobility. This is somewhat diminished when graphene is placed in contact with a substrate but values of up to $\mu = 4 \times 10^4$ cm^{-2} V^{-1} s^{-1} may be attainable.[29] If these values for carrier density and mobility can be achieved together in a working device, values of $n\mu = 1.2 \times 10^{17}$ V^{-1} s^{-1} are possible. This results in a value of $\sigma_{DC}/\sigma_{Op} = 330$. We note that this is not a fundamental limit but may represent the limit of what is practically attainable. Assuming that the transmittance is not effected by doping, four doped, randomly stacked monolayers should display a transmittance of $T = 91\%$.[60] Using eq 3, we can estimate the sheet resistance of such a film (assuming $n\mu = 1.2 \times 10^{17}$ V^{-1} s^{-1}) to be 11 Ω/□. This is close to the limit for ITO replacement, even in current driven devices.

Comparison with Other Nanomaterials. In Figure 1, we use eq 3 to plot the locus of limiting R_s and T values based on our calculated potential value of $\sigma_{DC}/\sigma_{Op} = 330$ (solid line). This curve is in line with what can be achieved with ITO ($T = 85-95\%$, $R_s = 10-100$ Ω/□). A maximum value of $\sigma_{DC}/\sigma_{Op} = 330$ compares favorably with that of carbon nanotube networks (maximum[20,21] $\sigma_{DC}/\sigma_{Op} = 35$) but is slightly inferior to that of silver nanowire networks (maximum[18] $\sigma_{DC}/\sigma_{Op} \approx 450$).

In addition, we note that even solution-cast graphene networks may be suitable for some transparent conductor applications. There are a number of applications such as electrostatic dissipation, electromagnetic interference shielding, touch screens, *etc.*, which do not require such high values of σ_{DC}/σ_{Op}. For such applications graphitic films, especially those deposited from solution, may play an important role. ITO costs \$2−30/m^2 for coatings with 90% transmittance. Films of high quality carbon nanotubes[15] with $T = 90\%$ (*ca.* \$1600/g, thickness ≈ 20 nm, equivalent to ∼10 mg/m^2) cost *ca.* \$15/m^2. Given that graphite costs *ca.* \$5−10/kg, solution processed films with 90% transmittance cost *ca.* 0.02¢/m^2 (thickness ≈ 10 nm, equivalent to ∼25 mg/m^2).[41] Given the magnitude of this cost differential, we feel solution-cast transparent graphitic films will certainly play a role in the electronics industry, just not as transparent electrodes.

CONCLUSION

We have analyzed data from the literature for transmittance and sheet resistance of graphene-based transparent conductors. We have calculated the ratio of DC to optical conductivity in each case. This parameter can be used as a figure of merit, allowing comparisons to be made between films and with other materials. We find that the best graphene films have σ_{DC}/σ_{Op} values clustered into three groups. We identify these as graphite-like films, graphene-like films, and networks of graphene flakes. The graphite films display the best properties with $\sigma_{DC}/\sigma_{Op} = 11$. However, we note that substrate-induced doping of graphene may result in values of $\sigma_{DC}/\sigma_{Op} = 330$, high enough for industrial transparent electrodes.

It is important to point out that the transparent electrode is only one small component in a device such as a light emitting diode or a solar cell. While emphasizing the importance of the transparent electrode, we must remember that design, fabrication, and integration will also play crucial roles in realizing practical devices. In addition, sheet resistance and transmittance are not the only properties of the transparent electrode that are important. Chemical resistance, lack of toxicity, adhesion, smoothness, work function, and a range of other factors are also essential. However, highly doped CVD grown graphene will fulfill many of these criteria. Thus we feel that if doping and mobility criteria can be met, graphene will play an important role in a number of device applications.

Acknowledgment. We acknowledge the Science Foundation Ireland funded collaboration (SFI Grant 03/CE3/M406s1) between Trinity College Dublin, University College Cork and Hewlett-Packard, Dublin Inkjet Manufacturing Operation, which has allowed this work to take place. J.N.C. is also supported by an SFI PI award.

Supporting Information Available: List of papers analyzed, including graphene type, optical, and DC conductivity and calculated conductivity ratio. This material is available free of charge *via* the Internet at http://pubs.acs.org.

REFERENCES AND NOTES

1. Gordon, R. G. Criteria for Choosing Transparent Conductors. *MRS Bull.* **2000**, *25*, 52.
2. Bhosle, V.; Prater, J. T.; Yang, F.; Burk, D.; Forrest, S. R.; Narayan, J. Gallium-Doped Zinc Oxide Films as Transparent Electrodes for Organic Solar Cell Applications. *J. Appl. Phys.* **2007**, *102*, 023501.
3. Yang, F.; Forrest, S. R. Organic Solar Cells Using Transparent SnO_2−F Anodes. *Adv. Mater.* **2006**, *18*, 2018+.
4. Meiss, J.; Riede, M. K.; Leo, K. Towards Efficient Tin-Doped Indium Oxide (ITO)-free Inverted Organic Solar Cells Using Metal Cathodes. *Appl. Phys. Lett.* **2009**, *94*, 013303.
5. O'Connor, B.; Haughn, C.; An, K. H.; Pipe, K. P.; Shtein, M. Transparent and Conductive Electrodes Based on Unpatterned, Thin Metal Films. *Appl. Phys. Lett.* **2008**, *93*, 223304.
6. Kang, M. G.; Kim, M. S.; Kim, J. S.; Guo, L. J. Organic Solar Cells Using Nanoimprinted Transparent Metal Electrodes. *Adv. Mater.* **2008**, *20*, 4408–4413.
7. Tvingstedt, K.; Inganas, O. Electrode Grids for ITO-free Organic Photovoltaic Devices. *Adv. Mater.* **2007**, *19*, 2893+.
8. The authors are collaborating with Hewlett Packard to develop transparent conductors for display applications. As part of this collaboration, HP specified 100 Ω/□ and 90% as the minimum requirements for transparent electrodes.
9. Geng, H. Z.; Kim, K. K.; So, K. P.; Lee, Y. S.; Chang, Y.; Lee, Y. H. Effect of Acid Treatment on Carbon Nanotube-Based Flexible Transparent Conducting Films. *J. Am. Chem. Soc.* **2007**, *129*, 7758.
10. Park, Y.-B.; Hu, L.; Gruner, G.; Irvin, G.; Drzaic, P. Late-News Paper: Integration of Carbon Nanotube Transparent Electrodes into Display Applications. *Soc. Inf. Disp. Symp. Dig.* **2008**, *39*, 37–7.

11. den Boer, W.; Smith, G. S. Dual Select Diode AMLCDs: A Path Towards Scalable Two-Mask Array Designs. *J. Soc. Inf. Disp.* **2005**, *13*, 199.
12. Rowell, M.; McGehee, M. Electrical Transport in Carbon nanotube FETs and Transparent Conductors - from Sparse Networks to Dense Films. *MRS Fall Meeting*, Boston, December 3, 2009.
13. Calnan, S.; Tiwari, A. N. High Mobility Transparent Conducting Oxides for Thin Film Solar Cells. *Thin Solid Films* **2010**, *518*, 1839.
14. Personal communication. McGehee, M., Stanford University, March 2010
15. Doherty, E. M.; De, S.; Lyons, P. E.; Shmeliov, A.; Nirmalraj, P. N.; Scardaci, V.; Joimel, J.; Blau, W. J.; Boland, J. J.; Coleman, J. N. The Spatial Uniformity and Electromechanical Stability of Transparent, Conductive Films of Single Walled Nanotubes. *Carbon* **2009**, *47*, 2466–2473.
16. Zhou, Y. H.; Zhang, F. L.; Tvingstedt, K.; Barrau, S.; Li, F. H.; Tian, W. J.; Inganas, O. Investigation on Polymer Anode Design for Flexible Polymer Solar Cells. *Appl. Phys. Lett.* **2008**, *92*, 233308.
17. Lee, J. Y.; Connor, S. T.; Cui, Y.; Peumans, P. Solution-Processed Metal Nanowire Mesh Transparent Electrodes. *Nano Lett.* **2008**, *8*, 689–692.
18. De, S.; Higgins, T.; Lyons, P. E.; Doherty, E. M.; Nirmalraj, P. N.; Blau, W. J.; Boland, J. J.; Coleman, J. N. Silver Nanowire Networks as Flexible, Transparent, Conducting Films: Extremely High DC to Optical Conductivity Ratios. *ACS Nano* **2009**, *3*, 1767–1774.
19. Hu, L.; Hecht, D. S.; Gruner, G. Percolation in Transparent and Conducting Carbon Nanotube Networks. *Nano Lett.* **2004**, *4*, 2513–2517.
20. Wu, Z. C.; Chen, Z. H.; Du, X.; Logan, J. M.; Sippel, J.; Nikolou, M.; Kamaras, K.; Reynolds, J. R.; Tanner, D. B.; Hebard, A. F.; Rinzler, A. G. Transparent, Conductive Carbon Nanotube Films. *Science* **2004**, *305*, 1273–1276.
21. Nirmalraj, P. N.; Lyons, P. E.; De, S.; Coleman, J. N.; Boland, J. J. Electrical Connectivity in Single-Walled Carbon Nanotube Networks. *Nano Lett.* **2009**, *9*, 3890–3895.
22. Wassei, J. K.; Kaner, R. B. Graphene, a Promising Transparent Conductor. *Mater. Today* **2010**, *13*, 52.
23. Kim, K. S.; Zhao, Y.; Jang, H.; Lee, S. Y.; Kim, J. M.; Kim, K. S.; Ahn, J.-H.; Kim, P.; Choi, J.-Y.; Hong, B. H. Large-Scale Pattern Growth of Graphene Films for Stretchable Transparent Electrodes. *Nature* **2009**, *457*, 706–710.
24. Li, X.; Zhang, G.; Bai, X.; Sun, X.; Wang, X.; Wang, E.; Dai, H. Highly Conducting Graphene Sheets and Langmuir-Blodgett Films. *Nat. Nano* **2008**, *3*, 538–542.
25. Eda, G.; Fanchini, G.; Chhowalla, M. Large-Area Ultrathin Films of Reduced Graphene Oxide as a Transparent and Flexible Electronic Material. *Nat. Nano* **2008**, *3*, 270–274.
26. Wu, J. B.; Agrawal, M.; Becerril, H. A.; Bao, Z. N.; Liu, Z. F.; Chen, S.; Peumans, P. Organic Light-Emitting Diodes on Solution-Processed Graphene Transparent Electrodes. *ACS Nano* **2010**, *4*, 43–48.
27. Wang, X.; Zhi, L.; Mullen, K. Transparent, Conductive Graphene Electrodes for Dye-Sensitized Solar Cells. *Nano Lett.* **2008**, *8*, 323–327.
28. Reina, A.; Jia, X.; Ho, J.; Nezich, D.; Son, H.; Bulovic, V.; Dresselhaus, M. S.; Kong, J. Large Area, Few-Layer Graphene Films on Arbitrary Substrates by Chemical Vapor Deposition. *Nano Lett.* **2009**, *9*, 30–35.
29. Li, X.; Zhu, Y.; Cai, W.; Borysiak, M.; Han, B.; Chen, D.; Piner, R. D.; Colombo, L.; Ruoff, R. S. Transfer of Large-Area Graphene Films for High-Performance Transparent Conductive Electrodes. *Nano Lett.* **2009**, *9*, 4359.
30. Green, A. A.; Hersam, M. C. Solution Phase Production of Graphene with Controlled Thickness *via* Density Differentiation. *Nano Lett.* **2009**, *9*, 4031–4036.
31. Blake, P.; Brimicombe, P. D.; Nair, R. R.; Booth, T. J.; Jiang, D.; Schedin, F.; Ponomarenko, L. A.; Morozov, S. V.; Gleeson, H. F.; Hill, E. W.; Geim, A. K.; Novoselov, K. S. Graphene-Based Liquid Crystal Device. *Nano Lett.* **2008**, *8*, 1704–1708.
32. Biswas, S.; Drzal, L. T. A Novel Approach to Create a Highly Ordered Monolayer Film of Graphene Nanosheets at the Liquid−Liquid Interface. *Nano Lett.* **2009**, *9*, 167–172.
33. Kim, Y.-K.; Min, D.-H. Durable Large-Area Thin Films of Graphene/Carbon Nanotube Double Layers as a Transparent Electrode. *Langmuir* **2009**, *25*, 11302–11306.
34. Cote, L. J.; Kim, F.; Huang, J. Langmuir Blodgett Assembly of Graphite Oxide Single Layers. *J. Am. Chem. Soc.* **2009**, *131*, 1043–1049.
35. Zhu, Y.; Cai, W.; Piner, R. D.; Velamakanni, A.; Ruoff, R. S. Transparent Self-Assembled Films of Reduced Graphene Oxide Platelets. *Appl. Phys. Lett.* **2009**, *95*, 103104.
36. Wu, J.; Becerril, H. A.; Bao, Z.; Liu, Z.; Chen, Y.; Peumans, P. Organic Solar Cells with Solution-Processed Graphene Transparent Electrodes. *Appl. Phys. Lett.* **2008**, *92*, 263302-1–263302-3.
37. Eda, G.; Lin, Y.-Y.; Miller, S.; Chen, C.-W.; Su, W.-F.; Chhowalla, M. Transparent and Conducting Electrodes for Organic Electronics from Reduced Graphene Oxide. *Appl. Phys. Lett.* **2008**, *92*, 233305-1–233305-3.
38. Cai, W.; Zhu, Y.; Li, X.; Piner, R. D.; Ruoff, R. S. Large Area Few-Layer Graphene/Graphite Films as Transparent Thin Conducting Electrodes. *Appl. Phys. Lett.* **2009**, *95*, 123115-1–123115-3.
39. Wang, X.; Zhi, L.; Tsao, N.; Tomovic, Z.; Li, J.; Muellen, K. Transparent Carbon Films as Electrodes in Organic Solar Cells. *Angew. Chem., Int. Ed.* **2008**, *47*, 2990–2992.
40. Becerril, H. c. A.; Mao, J.; Liu, Z.; Stoltenberg, R. M.; Bao, Z.; Chen, Y. Evaluation of Solution-Processed Reduced Graphene Oxide Films as Transparent Conductors. *ACS Nano* **2008**, *2*, 463–470.
41. De, S.; King, P. J.; Lotya, M.; O'Neill, A.; Doherty, E. M.; Hernandez, Y.; Duesberg, G. S.; Coleman, J. N. Flexible, Transparent, Conducting Films of Randomly Stacked Graphene from Surfactant-Stabilized, Oxide-free Graphene Dispersions. *Small* **2009**, *6*, 458.
42. Gunes, F.; Han, G. H.; Kim, K. K.; Kim, E. S.; Chae, S. J.; Park, M. H.; Jeong, H. K.; Lim, S. C.; Lee, Y. H. Large-Area Graphene-Based Flexible Transparent Conducting Films. *Nano* **2009**, *4*, 83–90.
43. Liang, Y.; Frisch, J.; Zhi, L.; Norouzi-Arasi, H.; Feng, X.; Rabe, J. P.; Koch, N.; Mullen, K. Transparent, Highly Conductive Graphene Electrodes from Acetylene-Assisted Thermolysis of Graphite Oxide Sheets and Nanographene Molecules. *Nanotechnology* **2009**, *20*, 434007.
44. Liu, Y.; Gao, L.; Sun, J.; Wang, Y.; Zhang, J. Stable Nafion-Functionalized Graphene Dispersions for Transparent Conducting Films. *Nanotechnology* **2009**, *20*, 465605.
45. Mattevi, C.; Eda, G.; Agnoli, S.; Miller, S.; Mkhoyan, K. A.; Celik, O.; Mostrogiovanni, D.; Granozzi, G.; Garfunkel, E.; Chhowalla, M. Evolution of Electrical, Chemical, and Structural Properties of Transparent and Conducting Chemically Derived Graphene Thin Films. *Adv. Funct. Mater.* **2009**, *19*, 2577–2583.
46. Wang, Y.; Chen, X. H.; Zhong, Y. L.; Zhu, F. R.; Loh, K. P. Large Area, Continuous, Few-Layered Graphene as Anodes in Organic Photovoltaic Devices. *Appl. Phys. Lett.* **2009**, *95*, 063302.
47. Zhao, L.; Zhao, L.; Xu, Y.; Qiu, T.; Zhi, L.; Shi, G. Polyaniline Electrochromic Devices with Transparent Graphene Electrodes. *Electrochim. Acta* **2009**, *55*, 491–497.
48. Geim, A. K. Graphene: Status and Prospects. *Science* **2009**, *324*, 1530–1534.
49. Geim, A. K.; Novoselov, K. S. The Rise of Graphene. *Nat. Mater.* **2007**, *6*, 183–191.
50. Park, S.; Ruoff, R. S. Chemical Methods for the Production of Graphenes. *Nat. Nanotechnol.* **2009**, *4*, 217–224.
51. Bourlinos, A. B.; Georgakilas, V.; Zboril, R.; Steriotis, T. A.; Stubos, A. K. Liquid-Phase Exfoliation of Graphite Towards Solubilized Graphenes. *Small* **2009**, *5*, 1841–1845.
52. Hernandez, Y.; Lotya, M.; Rickard, D.; Bergin, S. D.; Coleman, J. N. Measurement of Multicomponent Solubility Parameters for Graphene Facilitates Solvent Discovery. *Langmuir* **2010**, *26*, 3208.

53. Hernandez, Y.; Nicolosi, V.; Lotya, M.; Blighe, F. M.; Sun, Z. Y.; De, S.; McGovern, I. T.; Holland, B.; Byrne, M.; Gun'ko, Y. K.; *et al.* High-Yield Production of Graphene by Liquid-Phase Exfoliation of Graphite. *Nat. Nanotechnol.* **2008**, *3*, 563–568.
54. Hamilton, C. E.; Lomeda, J. R.; Sun, Z. Z.; Tour, J. M.; Barron, A. R. High-Yield Organic Dispersions of Unfunctionalized Graphene. *Nano Lett.* **2009**, *9*, 3460–3462.
55. Lotya, M.; Hernandez, Y.; King, P. J.; Smith, R. J.; Nicolosi, V.; Karlsson, L. S.; Blighe, F. M.; De, S.; Wang, Z. M.; McGovern, I. T.; *et al*. Liquid Phase Production of Graphene by Exfoliation of Graphite in Surfactant/Water Solutions. *J. Am. Chem. Soc.* **2009**, *131*, 3611–3620.
56. Berger, C.; Song, Z. M.; Li, X. B.; Wu, X. S.; Brown, N.; Naud, C.; Mayou, D.; Li, T. B.; Hass, J.; Marchenkov, A. N.; *et al.* Electronic Confinement and Coherence in Patterned Epitaxial Graphene. *Science* **2006**, *312*, 1191–1196.
57. Dressel, M.; Gruner, G. *Electrodynamics of Solids: Optical Properties of Electrons in Matter*; Cambridge University Press: Cambridge, U.K., 2002.
58. Dan, B.; Irvin, G. C.; Pasquali, M. Continuous and Scalable Fabrication of Transparent Conducting Carbon Nanotube Films. *ACS Nano* **2009**, *3*, 835–843.
59. De, S.; Lyons, P. E.; Sorrel, S.; Doherty, E. M.; King, P. J.; Blau, W. J.; Nirmalraj, P. N.; Boland, J. J.; Scardaci, V.; Joimel, J.; Coleman, J. N. Transparent, Flexible, and Highly Conductive Thin Films Based on Polymer-Nanotube Composites. *ACS Nano* **2009**, *3*, 714–720.
60. Nair, R. R.; Blake, P.; Grigorenko, A. N.; Novoselov, K. S.; Booth, T. J.; Stauber, T.; Peres, N. M. R.; Geim, A. K. Fine Structure Constant Defines Visual Transparency of Graphene. *Science* **2008**, *320*, 1308.
61. Lyons, P. E.; De, S.; Blighe, F.; Nicolosi, V.; Pereira, L. F. C.; Ferreira, M. S.; Coleman, J. N. The Relationship between Network Morphology and Conductivity in Nanotube Films. *J. Appl. Phys.* **2008**, *104*, 044302.
62. Yang, D.; Velamakanni, A.; Bozoklu, G.; Park, S.; Stoller, M.; Piner, R. D.; Stankovich, S.; Jung, I.; Field, D. A.; Ventrice, C. A.; Ruoff, R. S. Chemical Analysis of Graphene Oxide Films after Heat and Chemical Treatments by X-ray Photoelectron and Micro-Raman Spectroscopy. *Carbon* **2009**, *47*, 145–152.
63. Novoselov, K. S.; Geim, A. K.; Morozov, S. V.; Jiang, D.; Zhang, Y.; Dubonos, S. V.; Grigorieva, I. V.; Firsov, A. A. Electric Field Effect in Atomically Thin Carbon Films. *Science* **2004**, *306*, 666–669.
64. Novoselov, K. S.; Geim, A. K.; Morozov, S. V.; Jiang, D.; Katsnelson, M. I.; Grigorieva, I. V.; Dubonos, S. V.; Firsov, A. A. Two-Dimensional Gas of Massless Dirac Fermions in Graphene. *Nature* **2005**, *438*, 197–200.
65. Kuzmenko, A. B.; van Heumen, E.; Carbone, F.; van der Marel, D. Universal Optical Conductance of Graphite. *Phys. Rev. Lett.* **2008**, *100*, 117401.
66. Malard, L. M.; Pimenta, M. A.; Dresselhaus, G.; Dresselhaus, M. S. Raman Spectroscopy in Graphene. *Phys. Rep., Rev. Sect. Phys. Lett.* **2009**, *473*, 51–87.
67. Soule, D. E. Magnetic Field Dependence of the Hall Effect and Magnitoresistance in Graphite Single Crystals. *Phys. Rev.* **1958**, *112*, 698–707.
68. Edman, L.; Sundqvist, B.; McRae, E.; Litvin-Staszewska, E. Electrical Resistivity of Single-Crystal Graphite under Pressure: An Anisotropic Three-Dimensional Semimetal. *Phys. Rev. B* **1998**, *57*, 6227–6230.
69. Romero, H. E.; Shen, N.; Joshi, P.; Gutierrez, H. R.; Tadigadapa, S. A.; Sofo, J. O.; Eklund, P. C. N-Type Behavior of Graphene Supported on Si/SiO_2 Substrates. *ACS Nano* **2008**, *2*, 2037–2044.
70. Schedin, F.; Geim, A. K.; Morozov, S. V.; Hill, E. W.; Blake, P.; Katsnelson, M. I.; Novoselov, K. S. Detection of Individual Gas Molecules Adsorbed on Graphene. *Nat. Mater.* **2007**, *6*, 652–655.
71. Zheng, Y.; Ni, G. X.; Toh, C. T.; Zeng, M. G.; Chen, S. T.; Yao, K.; Ozyilmaz, B. Gate-Controlled Nonvolatile Graphene−Ferroelectric Memory. *Appl. Phys. Lett.* **2009**, *94*, 163505.